Environmental Epigenetics, 2025, **11(1)**, 1–14
DOI: https://doi.org/10.1093/eep/dvaf010
Advance Access Publication 24 April 2025
**Research Article**

# Prenatal per- and polyfluoroalkyl substance exposures and DNA methylation among newborns in the Environmental influences on Child Health Outcomes program

**Rose Schrott[1], Christine Ladd-Acosta[1], Vasantha Padmanabhan[2], Dana Boyd Barr[3], Carrie V. Breton[4], Andres Cardenas[5], Courtney C. Carignan[6], Dana Dabelea[7], Anne L. Dunlop[8], Danielle M. Fallin[9], Marie-France Hivert[10], Ellen M. Howerton[1], Anna K. Knight[8], Emily Oken[10], Alicia K. Peterson[11], Michael C. Petriello[12], Douglas Ruden[13], Rebecca J. Schmidt[14], Alicia K. Smith[8], Anne P. Starling[7,15], Ivana V. Yang[16], Yeyi Zhu[11], Jaclyn M. Goodrich,[17,†,*] on behalf of the ECHO Cohort Consortium**

[1]Department of Epidemiology, Johns Hopkins Bloomberg School of Public Health, Baltimore, MD 21205, United States
[2]Department of Pediatrics, University of Michigan, Ann Arbor, MI 48109, United States
[3]Gangarosa Department of Environmental Health, Rollins School of Public Health, Emory University, Atlanta, GA 30322, United States
[4]Department of Population and Public Health Sciences, University of Southern California, Los Angeles, CA 90033, United States
[5]Department of Epidemiology and Population Health, Stanford University, Stanford, CA 94305, United States
[6]Department of Food Science and Human Nutrition, Department of Pharmacology and Toxicology, Michigan State University, East Lansing, MI 48824, United States
[7]Lifecourse Epidemiology of Adiposity and Diabetes (LEAD) Center, University of Colorado Anschutz Medical Campus, Aurora, CO 80045, United States
[8]Department of Gynecology and Obstetrics, School of Medicine, Emory University, Atlanta, GA 30322, United States
[9]Rollins School of Public Health, Emory University, Atlanta, GA 30322, United States
[10]Division of Chronic Disease Research Across the Lifecourse (CoRAL), Department of Population Medicine, Harvard Medical School, Harvard Pilgrim Health Care Institute, Boston, MA 02215, United States
[11]Division of Research, Kaiser Permanente Northern California, Pleasanton, Pleasanton 94588 United States
[12]Department of Pharmacology, Wayne State University, Detroit, MI 48201, United States
[13]Department of Obstetrics and Gynecology, Institute of Environmental Health Sciences, Wayne State University, Detroit, MI 48201, United States
[14]Department of Public Health Sciences and the MIND Institute, University of California Davis School of Medicine, Davis, CA 95817, United States
[15]Department of Epidemiology, Gillings School of Global Public Health, University of North Carolina at Chapel Hill, Chapel Hill, NC 27599, United States
[16]Department of Biomedical Informatics, University of Colorado Anschutz Medical Campus, Aurora, CO 80045, United States
[17]Department of Environmental Health Sciences, University of Michigan, Ann Arbor, MI 48109, United States

[†]See appendix for full list of collaborators.
*Corresponding author. Department of Environmental Health Sciences, University of Michigan, 1415 Washington Heights, Ann Arbor, MI 48109, USA.
E-mail: gaydojac@umich.edu

## Abstract

Gestation is a vulnerable window when exposure to per- and polyfluoroalkyl substances (PFAS) may impact child development and health. Epigenetic modification, including DNA methylation (DNAm), may be one mechanism linking prenatal PFAS exposure to offspring outcomes. We tested associations between prenatal PFAS and newborn DNAm in 1017 participants from 6 cohorts in the US Environmental influences on Child Health Outcomes consortium. Concentrations of PFAS [perfluorooctanesulfonic acid (PFOS), perfluorooctanoic acid (PFOA), perfluorohexanesulfonic acid (PFHxS), perfluorononanoic acid (PFNA), and perfluorodecanoic acid] were measured in maternal serum or plasma. DNAm was quantified in newborn dried blood spot or umbilical cord blood leukocytes using the Infinium HumanMethylation450 (450K) or MethylationEPIC (EPIC) arrays. We tested associations between prenatal PFAS and neonatal blood DNAm on the 450K ($n = 772$) and EPIC ($n = 245$) arrays; results were meta-analysed across the platforms. Regional changes in DNAm were investigated, and findings were checked for replication in the Michigan Mother–Infant Pairs (MMIP) cohort ($n = 140$). Following correction for false discovery rate ($q = 0.1$ for meta-analyses), we identified an association between PFHxS and one cytosine–guanine (CpG) mapped to *CASC3* ($q = 0.065$) that replicated in MMIP ($P = .006$). PFOS was associated with six CpG sites, of which five were mapped to the genes *KIAA1841*, *ABR*, *LEP*, *SERPINA1*, and *LOXL1*. One differentially methylated region (DMR) was associated with prenatal PFOA

Received 7 August 2024; Revised 6 February 2025; Accepted 21 April 2025

exposure, and one DMR was associated with PFOS exposure. In this multicohort analysis including a diverse group from the USA, PFOA, PFOS, PFHxS, and PFNA exposures in pregnancy were associated with offspring DNAm, and the implications for children's health merit further exploration.

**Keywords:** per- and polyfluoroalkyl substances; perfluorinated chemicals; epigenetics; epigenomics; children's health; developmental origins of health and disease; DNA methylation

## Introduction

Per- and polyfluoroalkyl substances (PFAS) are a class of synthetic chemicals of concern to public health. PFAS have been used to make fluoropolymer coatings for products due to their flame-retardant and stain-, water-, and grease-resistant properties. Given these properties, PFAS are widely found in products used by the general population such as cookware, carpets, furniture, shoes, dental floss, and food packaging [1–5]. PFAS are also a key component of aqueous film-forming foams used at sites such as airports and military bases [6]. PFAS contaminate drinking water and groundwater throughout the USA; it is now estimated that at least 45% of US drinking water sources contain PFAS [7–9]. Although awareness of the hazards of PFAS on public health as well as the number of PFAS regulations have rapidly increased in the USA and globally in the past few years [10, 11], legacy exposures to banned PFAS still continue due to their long half-lives in the environment and in people [12–14]. In addition, the concerning toxicity of emerging and replacement PFAS is becoming apparent [15, 16].

While PFAS act as multisystem toxicants and elicit harmful health effects at all stages of life, exposure during pregnancy, a sensitive period when organs are differentiating, merits particular consideration. PFAS have the ability to cross and accumulate in the placenta during pregnancy [17, 18], and exposure has been associated with a suite of adverse health outcomes at birth and across childhood. Specifically, prenatal exposure to PFAS has been associated with preterm birth [19], lower birth weight [20], and long-term effects on children including increased mid-childhood adiposity among girls [21] and increased body mass index (BMI) in early adulthood [22]. There is robust evidence to support that prenatal PFAS exposure has been associated with cholesterol-related outcomes including cardio-metabolic indicators [23, 24] and adverse plasma lipid concentrations [25] in cord blood, as well as immune system dysregulation [26] in children. Other studies have found neurodevelopmental impacts from prenatal PFAS exposure, although findings are not consistent [27–30]. Epigenetic perturbation may be one biological mechanism linking gestational PFAS exposure to children's outcomes. Environmental exposures, especially during early gestation, perturb epigenetic programming and metabolic homeostasis, setting the stage for altered foetal growth and ultimately disease development later in life. DNA methylation (DNAm) is one mechanism of epigenetic regulation that is stable across time at many cytosine–guanine (CpG) dinucleotides, although it is responsive to the environment [31]. The epigenome, including the DNA methylome, is dynamic and vulnerable to exogenous exposures during embryogenesis due to the waves of epigenetic reprograming that occur post-fertilization and post-implantation, which can lead to epigenetic dysregulation [32].

There is a growing body of literature focused on the relationship between PFAS exposure and epigenetic regulation, and particularly, DNAm (reviewed in [33, 34]). Associations between PFAS and altered epigenetics have been observed at various life stages of exposure in rodents, zebrafish, and humans [33]. Epidemiologic studies of prenatal PFAS exposure have identified DNAm changes at birth and throughout childhood [34]. Although most studies have been underpowered, three notable epigenome-wide studies provided evidence for alteration of DNAm in genes involved in growth, lipid metabolism, immune function, and more. The Upstate New York Infant Development Screening (Upstate KIDS) study ($n = 597$) based in New York reported a small number of statistically significant associations between prenatal perfluorooctanoic acid (PFOA) and perfluorooctanesulfonic acid (PFOS) exposure and DNAm in neonatal blood spots assessed via the Infinium MethylationEPIC (EPIC) array, although this study was limited by analysis of only two PFAS measured at the time of birth [35]. The Healthy Start cohort, which is also included in the present study, reported associations between 5 PFAS and cord blood DNAm at multiple genes including genes involved in cardiometabolic function among 583 newborns [23]. Work from the Health Outcomes and Measures of the Environment Study identified DNAm changes in cord blood at birth that persisted into childhood, as measured in peripheral blood leukocytes at 12 years of age, and that were associated with prenatal exposure to PFOS, PFOA, perfluorohexanesulfonic acid (PFHxS), and perfluorononanoic acid (PFNA) [36].

Most studies use methods that capture total methylation at cytosine residues, but hydroxymethylation and methylation are separate modifications with distinct roles in gene regulation [37]. In the Michigan Mother–Infant Pairs (MMIP) cohort, associations between PFAS with methylation and hydroxymethylation were assessed separately, and dozens to thousands of CpG sites were associated with six PFAS when these modifications were considered separately instead of combined [23, 38].

Research to date clearly indicates that prenatal PFAS exposures have the potential to modify DNAm in offspring and that these modifications may persist in childhood. However, the heterogeneity of results across studies hinders our ability to identify replicable biomarkers of prenatal exposure that can be used to understand past exposures or underlying biological pathways of concern to target for prevention or intervention strategies to protect against PFAS toxicity. Our objective was to conduct a multicohort analysis to identify genes and their biological pathways in offspring that are differentially methylated by prenatal exposure to five individual PFAS: PFOS, PFOA, PFHxS, perfluorodecanoic acid (PFDA), and PFNA. We hypothesized that gestational exposures to each PFAS would be associated with altered DNAm in the offspring in genes relevant to early life growth, metabolic programming, and immune function. To conduct this analysis, we pooled data from six cohorts—The Healthy Start Study, the Atlanta ECHO Cohort of Emory University, the Maternal and Developmental Risks from Environmental and Social Stressors (MADRES) Study, the New Hampshire Birth Cohort Study, Project Viva, and the Archive for Research on Child Health (ARCH). These cohorts are part of the Environmental influences on Child Health Outcomes (ECHO) consortium [39] and measured at least two prenatal PFAS in pregnancy samples and DNAm in offspring samples collected at birth. ECHO comprises multiple US-based cohorts from diverse racial, ethnic, and socioeconomic backgrounds. This provides rich

opportunities to explore the generalizability of our findings across other populations in the country and around the globe.

# Methods

## Study population

The ECHO cohort is a national program of more than 60 observational sites that is dedicated to understanding the role of the environment in child health and development [39–44]. We included any ECHO participants that had the following: DNAm assessment via the Infinium HumanMethylation450 (450K) or EPIC in neonatal samples collected at or near the time of birth (e.g. cord blood and neonatal blood spots) and PFAS exposure assessment using maternal serum or plasma samples collected during pregnancy. There were no exclusion criteria based on initial cohort participation. This study used data available through the ECHO data repository as of the 31 March 2023, data lock date. The study protocol was approved by the single ECHO institutional review board (IRB). Original data collection from each cohort was approved by the cohorts' local IRBs, and all study participants (parents) provided informed consent.

Participants from this study were born between 1999 and 2019 and were recruited from six participating ECHO cohorts: The Healthy Start Study, the Atlanta ECHO Cohort of Emory University, the MADRES Study, the New Hampshire Birth Cohort Study, Project Viva, and ARCH. There were 1017 participants with DNAm and exposure data for four PFAS (PFNA, PFOA, PFOS, and PFHxS). For one additional PFAS, PFDA, there were 1000 total participants with DNAm and exposure.

## Replication cohort

We sought to replicate statistically significant results in a non-ECHO cohort with the same types of data. The MMIP, with first trimester PFAS data and DNAm in cord blood via the EPIC array, was selected as the replication cohort. MMIP is a birth cohort study based out of the University of Michigan Von Voigtlander Women's Hospital. Participants ($n = 140$) were recruited between 2010 and 2019 during their first prenatal visit if they were at least 18 years old, had a singleton pregnancy, and were between 8 and 14 weeks of gestation. Other details about the cohort, including details on PFAS and epigenetic analysis, have been previously detailed [38, 45, 46]. All participants provided informed, written consent prior to study enrollment. The University of Michigan Medical School IRB approved all study procedures.

## Per- and polyfluoroalkyl substance analysis

For each PFAS analyte, when more than one measurement per mother was available, we retained the measurement taken from the earliest trimester available. We included PFAS measurements from maternal plasma or serum collected during pregnancy; 31.9% of participants had PFAS measured in the first trimester, 30.9% in the second, and 37.3% in the third trimester. The laboratories conducting the analyses included the Wadsworth Center-Human Health Exposure Analysis Resource Laboratory and the Centers for Disease Control and Prevention. Although the number of PFAS analysed varied by cohort, we included PFAS that were measured and widely detected in all cohorts [>50% of samples above the limit of detection (LOD)]: PFOS, PFOA, PFHxS, PFNA, and PFDA. PFAS analysis in the replication cohort was performed using first trimester plasma samples at NSF International as previously described [38]. Analytes with measures below the LOD were imputed using cohort-specific LOD divided by the square root of 2. Since PFAS concentrations were right-skewed, values were natural log-transformed prior to analysis [27, 47].

## Biospecimen collection and DNA methylation assessment

Cohorts included in the present study collected cord blood or newborn dried blood spots through approved site-specific protocols. DNAm was measured using the 450K or EPIC arrays (Illumina, San Diego, USA). Raw data files from each ECHO site with DNAm data were imported into the minfi processing pipeline in R to calculate 'beta' values for each probe and sample; beta values (estimating the proportion of DNAm at each locus from 0 to 1) were calculated as previously described [48]. Sample and probe-level filters were applied to the data [48]. Briefly, samples were removed if there were discrepancies between reported and predicted sex, there was a low overall signal intensity, duplicates were present, >1% of probes for the sample had a detection $P$-value > .05 (compared to background signal), or >1% of probes had a bead count <3. Probes were removed if >1% of samples had a detection $P$-value > .05, >1% of samples had bead count <3, probes were cross reactive, or if there was a known single-nucleotide polymorphism at the CpG site queried. Background correction and within-sample normalization were performed on the filtered data sets for each methylation platform using the noob function in *minfi* as described [48]. Finally, additional sample filters were applied to the noob-corrected data sets based on age and tissue-type discrepancies to achieve clean data sets for each platform for analysis [48].

## Confounders/covariates

Covariate data harmonized across cohorts included self-reported maternal race and ethnicity, maternal education, maternal tobacco use, maternal BMI, parity, maternal age, and child sex. These data were obtained from participant report on sociodemographic questionnaires or via medical records. We included self-reported race and ethnicity as covariates because of concerns that each could independently associate with both prenatal PFAS exposure and DNAm, though this may be a proxy for the impacts of structural and environmental racism and not biological differences. Technical covariates in statistical models included DNAm batch and blood cell composition estimates. For cord blood biospecimens, we adjusted for CD4+ T cells, CD8+ T cells, granulocytes, monocytes, natural killer cells, and red blood cells, and for dried blood spot biospecimens, we adjusted for CD4+ T cells, CD8+ T cells, granulocytes, monocytes, and natural killer cells.

## Statistical approach

*1. Descriptive statistics*. R version 4.2 was used for statistical analyses unless otherwise specified. Descriptive statistics were calculated for continuous and categorical variables across all participants for each cohort. For PFAS concentrations, we calculated the geometric mean, median, IQR, minimum, and maximum for each analyte, and all PFAS data were natural log transformed prior to running analyses.

When missingness was present among demographic variables and was found to be unrelated to the exposures, we applied the following imputation method: using the first step of multiple imputations for categorical variables with missingness, the distributions of the complete data were defined, and random samples were drawn from these distributions, as previously described [38], with the major category imputed. For continuous variables with missingness (maternal BMI), we imputed using the cohort-specific mean.

2. *Epigenome-wide association testing*. Epigenome-wide association tests between prenatal PFAS and DNAm were performed separately for the 450K and EPIC arrays. Among those with PFNA, PFHxS, PFOA, and PFOS data, 772 participants had DNAm data from cord blood on the 450K array. The remaining 245 dried blood spot ($n = 147$) and cord blood ($n = 98$) samples were analysed on the EPIC array separately by tissue type. Among those with PFDA, there were 772 participants with cord blood DNAm data measured on the 450K array, and 228 participants measured on the EPIC array. We used a linear regression model of the beta methylation value at each locus as the dependent variable, and PFAS exposure, maternal race, maternal ethnicity, parity, maternal BMI, child sex, DNAm batch, and tissue-specific cell composition estimates as independent variables. These variables were selected *a priori* by using a directed acyclic graph and prior knowledge of variables that strongly influence the DNA methylome assessed via Infinium arrays (cell type composition, batch, and sex) and potential confounders in the relationship between PFAS exposures and DNAm (maternal race and ethnicity as proxies for structural and environmental racism, parity, and maternal early- or pre-pregnancy BMI). We implemented modelling using the *lmFit()* function from the *limma* R package for each of the DNAm probes that passed quality control [49]. We then calculated the genomic inflation factor, lambda, to ensure reasonable control of genomic inflation [49]. After completing association testing for each array and tissue type individually, we meta-analysed data across the 3 EWAS results using an inverse variance weighted approach with the METAL software on the 361 610 probes that were in common across the 450K and EPIC arrays [50]. False discovery rate (FDR) was computed using the Benjamini–Hochberg method [51], and $q < 0.1$ was taken to be significant. CpG sites were annotated to genes using human assembly GRCh37/hg19. For EPIC-only analyses, we used the same approach in METAL to meta-analsze EWAS results from the cord blood and dried blood spot analyses, and $q < 0.05$; a more stringent cut-off was used given the secondary nature of these analyses.

3. *ipDMR*.Differentially methylated region (DMR) analyses were performed using the *ipDMR()* function from the *ENmix* R package [52]. Briefly, ipDMR identifies DMRs based on user-provided association *P*-values for individual CpG sites from an epigenome-wide study. Firstly, the function calculates a *P*-value for the interval bordered by two adjacent CpG sites within the specified value of 1000 base pairs. After performing the Benjamini–Hochberg procedure on the interval *P*-values, we selected those that had an FDR < 0.05. All nearby significant intervals and CpGs were then joined as long as the gap between CpGs was <1000 base pairs, and a *P*-value for the combined region was recalculated using the original *P*-value for all CpGs in the region. A final FDR correction ($q < 0.05$) was performed on the region *P*-values to obtain the FDR-adjusted *P*-value. Finally, we filtered for DMRs that consisted of three or more consecutive CpG sites.

4. *Gene Ontology (GO) analysis*. GO analyses were performed using the *gometh()* function from the *missMethyl* R package to determine whether there was any enrichment for gene pathways among CpG sites associated with exposures [53]. This package takes into account the bias often present in gene set testing for methylation array data given that a subset of CpG sites are annotated to more than one gene, as well as selection biases where different numbers of probes per gene are present on different array technologies [53]. We limited the analysis to PFAS that were significantly associated ($q < 0.05$) with any sites in the previous analyses, and we inputted the top 1000 CpG sites by raw *P*-value. In addition to GO analysis, we looked up whether any of the genes with differentially methylated CpG sites or regions by PFAS had previously reported PFAS–gene interactions in the Comparative Toxicogenomics Database [54] or whether any of these genes were predicted or known PPAR target genes given the established relationship between PFAS and PPARs [55–58].

5. *Replication cohort*. Beta methylation values from CpG sites significantly associated (FDR < 0.05) with at least one PFAS in the ECHO analysis were extracted from the MMIP EPIC array dataset, preprocessed as previously described [38]. Associations between each PFAS (log2 transformed) and total DNAm at these loci were tested in 140 MMIP participants using linear regression, adjusting for maternal race, parity, child sex, maternal smoking, batch, and estimated cord blood cell type proportions.

# Results

## Study demographics

There were 1017 participant dyads who met the inclusion criteria for this study, having PFAS measured in maternal serum ($n = 823$) or plasma ($n = 194$) collected during pregnancy, and DNAm measured in cord blood ($n = 870$) or dried blood spots ($n = 147$; Fig. 1). Demographic information for the participants can be found in Table 1. The mean maternal age of the participants was 28.9 years of age, and the majority of babies were born at full term with a mean gestational age of 39 weeks. There was a roughly even split between those who were previously nulliparous (50.4%) and those who had other children (48.5%). The majority of mothers were non-smokers (84.1%), white (75.1%), and non-Hispanic (75.1%), with an education of at least some college (66.3%). Mothers were on average categorized as slightly overweight with a mean pre-pregnancy BMI of 26.34 kg/m$^2$. Among newborns, 48.6% were female and 51.4% were male. There was a slightly smaller population with PFDA data ($n = 1000$ participants), although the demographic information was nearly identical to that of the full study population (Supplementary Table S1).

## Per- and polyfluoroalkyl substance exposures

There were 1017 participants with PFHxS, PFOS, PFOA, and PFNA concentrations measured from maternal blood in pregnancy included in this study, and 1000 participants with PFDA concentrations. Based on the cohort-specific median for each analyte, concentrations of PFOS and PFOA were highest in Project Viva. PFHxS was highest in ARCH and Project Viva. Concentrations of PFNA and PFDA were highest in the New Hampshire Birth Cohort Study, though PFNA and PFDA were low in all cohorts (medians <1 ng/mL; Supplementary Table S2). The total study population geometric mean, median with interquartile range (IQR), and minimum and maximum measurement for each PFAS analyte can be found in Table 2.

## Meta-analysis findings

We conducted an epigenome-wide association study ($n = 361\,610$ CpG sites) examining associations between prenatal PFAS exposure and DNAm measured in neonatal blood specimens. Lambda values for the meta-analyses were as follows: PFOA = 1.15, PFOS = 1.28, PFDA = 0.99, PFNA = 0.95, and PFHxS = 0.94. Following FDR correction ($q \leq 0.1$), there were seven CpG sites where we detected an association between prenatal PFAS exposure and blood DNAm at birth (Table 3). Specifically, PFOS concentrations were associated with six CpG sites mapped to the genes *KIAA1841* ($q = 0.030$), *ABR* ($q = 0.030$), *LEP* ($q = 0.030$), *SERPINA1* ($q = 0.056$), *LOXL1* ($q = 0.068$), and cg22777441 ($q = 0.068$) which was not annotated to a gene. The direction of effect was positive for all six of these CpG sites (effect sizes in adjusted models = 0.0053, 0.0065,

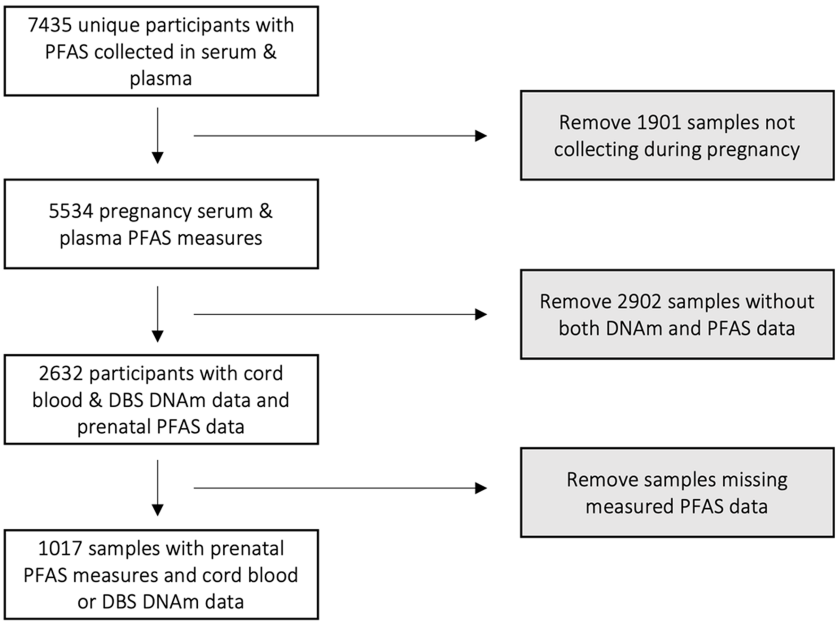


**Figure 1.** Participants included in the analysis.
DBS, dried blood spot.

0.0054, 0.005, 0.004, and 0.0067, respectively); effect sizes correspond to a change in the proportion of methylation per one-unit increase in natural-log transformed PFAS concentration. Three of these CpG sites were within or near CpG Islands. Tests for heterogeneity did not display major heterogeneity across meta-analysed results for five of the six CpG sites, with a heterogeneity $P > .05$ for those five sites, and $I^2$ statistics from 0% to 12.1% (Table 3). The CpG site annotated to *LEP*, had a heterogeneity $P = .05$ and an $I^2$ statistic of 65.9. Additionally, PFHxS concentrations were associated with DNAm at one CpG site mapped to the gene *CASC3* ($q = 0.065$). The direction of effect was positive (effect size = 0.0027 in adjusted models), and tests for heterogeneity were null ($I^2 = 1.39\%$ and heterogeneity *P*-value = .38).

## Differentially methylated regions

We performed DMR analysis to identify regional methylation changes associated with PFAS exposure. After applying the *ipDMR* function and filtering for DMRs that contained two or more CpG sites in a 1000 base pair region, we identified two DMRs associated ($q < 0.05$) with prenatal PFAS exposure (Table 4). Prenatal PFOA exposure was inversely associated with one DMR located in the South Shore of a CpG island and annotated to the gene *SSR3*. PFOS exposure was positively associated with DNAm at five CpG sites comprising a DMR annotated to the gene *ZDHHC14*.

## Per- and polyfluoroalkyl substance and DNA methylation: Infinium MethylationEPIC-only analysis

Given that there are hundreds of thousands of CpG sites covered on the EPIC array that are not included on the 450K array, we examined the associations between prenatal PFAS exposure and DNAm in the subset of 245 participants who had DNAm measured on the EPIC array separately. Lambda values for the EPIC-only analyses were as follows: PFOS = 1.67, PFNA = 0.88 PFOA = 1.13, PFHxS = 1.1, and PFDA = 0.81. From this epigenome-wide analysis, we identified 1 CpG site significantly associated with prenatal PFNA exposure; 1 CpG site significantly associated with PFOA exposure, and 133 CpG sites significantly associated with PFOS exposure (Table 5, $q < 0.05$). The CpG site associated with PFNA was unique to the EPIC array, while the CpG site associated with PFOA was present on both the EPIC and 450K arrays. Of the 133 PFOS-associated sites, 107 were unique to the EPIC array, while the remainder were present on both the EPIC and 450K arrays. The direction of effect was positive for the majority (130/133) of the CpG sites associated with prenatal PFOS, with effect sizes ranging from –0.0113 to 0.0253. The direction of effect was positive for the CpG sites that were associated with prenatal PFNA and PFOA exposures, with effect sizes of 0.0305 and 0.0104, respectively.

We performed GO analyses to identify functional pathways associated with the CpG sites that were significantly associated with prenatal PFOS and PFDA exposure in the EPIC-only analyses. No GO terms were significantly enriched at a $q < 0.05$ (see top GO terms in Supplementary Tables S3, S4, and S5).

## Replication cohort

We assessed whether associations between PFAS and DNAm replicated in an independent cohort with first trimester PFAS concentrations and cord blood leukocyte DNAm data quantified via the EPIC array. The replication cohort, MMIP, consisted of 140 participants (Supplementary Table S6). Median PFAS concentrations for PFOA, PFNA, and PFDA were similar to the ECHO median (Supplementary Table S7), while PFHxS and PFOS were substantially higher (medians 3.29 and 5.52 ng/mL, respectively). Among CpG sites associated with PFAS in the meta-analysis ($q \leq 0.1$, in Table 3), six were available in the MMIP dataset. One was significant in MMIP—the association between PFHxS and CASC3 methylation (probe ID cg27426500, $P = .006$); however, it was in the opposite direction (Supplementary Table S8). Seven of the loci associated with PFOS in the EPIC-only analysis were also significant in MMIP ($P < .05$, Supplementary Table S8). These sites were in intergenic regions (probe IDs cg26046406 and cg10626792) and *FGGY, ODZ4, SLC47A1, WDFY3*, and *TMEM131* (probe IDs cg15591629, cg03825175, cg05947984, cg04355093, and cg17238473, respectively).

**Table 1.** Study population characteristics

| Characteristic | $n = 1017$ |
|---|---|
| Maternal age at delivery (years), mean (SD) | 28.94 (6.2) |
| Gestational age at birth (weeks), mean (SD) | 39.04 (1.4) |
| Parity | |
| Nulliparous | 513 (50.4) |
| Multiparous | 493 (48.5) |
| Missing | 11 (1.1) |
| Maternal smoking during pregnancy | |
| No | 855 (84.1) |
| Yes | 68 (6.7) |
| Missing | 94 (9.2) |
| Maternal race | |
| Asian | 30 (2.9) |
| Black | 165 (16.2) |
| White | 764 (75.1) |
| More than one race | 21 (2.1) |
| Any other | 26 (2.6) |
| Missing | 11 (1.1) |
| Maternal ethnicity | |
| Hispanic | 251 (24.7) |
| Non-Hispanic | 764 (75.1) |
| Missing | 2 (0.2) |
| Child sex | |
| Female | 494 (48.6) |
| Male | 523 (51.4) |
| Maternal pre-pregnancy BMI in kg/m$^2$, mean (SD) | 26.34 (6.74) |
| Maternal education | |
| Less than high school | 150 (14.7) |
| High school or GED | 166 (16.3) |
| Some college and above | 674 (66.3) |
| Missing | 27 (2.7) |
| Specimen collection trimester for PFAS analysis | |
| First | 324 (31.9) |
| Second | 314 (30.9) |
| Third | 379 (37.3) |

Data shown are *n* (%) except where indicated.
GED, general educational development

**Table 2.** PFAS concentrations (ng/mL) in pregnancy samples

| | *n* | Geometric mean | Median | IQR | Min | Max |
|---|---|---|---|---|---|---|
| PFHxS | 1017 | 1.08 | 1.1 | 0.6, 2 | 0.07 | 25.5 |
| PFOS* | 1017 | 3.47 | 3 | 1.6, 7.39 | 0.029 | 134 |
| PFOA* | 1017 | 1.18 | 1.27 | 0.67, 2.27 | 0.015 | 22.4 |
| PFNA | 1017 | 0.36 | 0.4 | 0.26, 0.60 | 0.014 | 4.3 |
| PFDA | 1000 | 0.09 | 0.08 | 0.07, 0.20 | 0.022 | 3.5 |

*Total PFOS and PFOA.

## Discussion

In this analysis of six US-based birth cohorts, we identified associations between prenatal exposure to PFOA, PFOS, PFHxS, and PFNA with DNAm at select CpG sites or regions in newborn samples (umbilical cord blood or neonatal blood spots). In the meta-analysis of all cohorts, PFOS was associated with six differentially methylated sites ($q < 0.1$) and 1 DMR ($q < 0.05$). PFHxS was associated with one differentially methylated CpG site ($q < 0.01$), and PFOA was associated with one DMR ($q < 0.05$). The PFHxS-associated site in *CASC3* replicated in MMIP, but in the opposite direction.

In the analysis including only the cohorts with EPIC array data, PFOA and PFNA were each associated with 1 CpG site, while PFOS was associated with 133 CpG sites ($q < 0.05$). Of these CpG sites, the site associated with PFNA was unique to the EPIC array, as were

**Table 3.** Associations between PFAS and DNAm (FDR < 0.1), meta-analysis results

| PFAS | Gene name | Probe ID | Genomic location* | Relation to CpG island | Effect estimate | SE | P-value | FDR (*q*-value) | Direction | Heterogeneity $I^2$ | Heterogeneity *P*-value |
|---|---|---|---|---|---|---|---|---|---|---|---|
| PFHxS | *CASC3* | cg27426500 | chr17:38 327 194 | Open Sea | 0.0027 | 5.00E−04 | 1.80E−07 | 0.065 | +++ | 1.93 | 0.38 |
| PFOS | *KIAA1841* | cg06528150** | chr2:61 293 470 | Island | 0.005 | 0.001 | 8.94E−08 | 0.030 | +++ | 0 | 0.62 |
| PFOS | *ABR* | cg14381452 | chr17:973 621 | N. Shore | 0.007 | 0.001 | 2.36E−07 | 0.030 | +++ | 12.1 | 0.32 |
| PFOS | *LEP* | cg16683741 | chr7:127 891 959 | Open Sea | 0.005 | 0.001 | 2.47E−07 | 0.030 | −++ | 65.9 | 0.05 |
| PFOS | *SERPINA1* | cg25042671 | chr14:94 849 061 | Open Sea | 0.005 | 0.001 | 6.15E−07 | 0.056 | +++ | 11.1 | 0.32 |
| PFOS | | cg22777441 | chr12:130 411 334 | Open Sea | 0.004 | 0.001 | 1.13E−06 | 0.068 | +++ | 0 | 0.86 |
| PFOS | *LOXL1* | cg24168641 | chr15:74 219 645 | Island | 0.007 | 0.001 | 1.08E−06 | 0.068 | +++ | 0 | 0.88 |

*Locations are according to genome build GRCh37/hg19.
SE, standard error.
++ refers to concordance in the direction of effect across the meta-analysed datasets.
**CpG site passes Bonferroni significance threshold 1.38e−07.

**Table 4.** Associations between PFOA and DNAm at regions of consecutive CpG sites ($q$-value < 0.05)

| PFAS | Genomic location* | Gene name | Relation to CpG island | P-value | FDR ($q$-value) | Number of CpG sites | Probe IDs for CpG sites included in the DMR | Direction** |
|---|---|---|---|---|---|---|---|---|
| PFOA | chr3:156 273 297–156 273 458 | SSR3 | S. Shore | 9.27E–09 | 1.11E–07 | 3 | cg03885646, cg14741143, cg14929208 | — |
| PFOS | chr6:157 931 791–157 932 180 | *ZDHHC14* | Open Sea | 2.71E–13 | 5.68E–12 | 5 | cg00017931, cg01174743, cg03344384, cg09981914, cg20988098 | +++++ |

*Locations are according to genome build GRCh37/hg19.
**Direction indicates the direction of the association between the PFAS and each CpG site included in the DMR.

107 of the 133 sites associated with PFOS. The CpG site associated with PFOA, as well as the remaining 26 CpG sites associated with PFOS, were found on both the EPIC and 450K arrays. Seven of the sites associated with PFOS replicated in MMIP. Of the 27 total CpG sites that were in common across both platforms, none of them showed up as significant in our meta-analysis. This may be due to cohort differences in PFAS exposure, where the association was strongest for this chemical in the smaller subset of cohorts that had measures on the EPIC array which were then diluted out when analysed in the larger sample despite our best efforts to adjust for cohort differences in the meta-analysis. The majority (107/133) of CpG sites that were significantly associated with prenatal PFOS exposure, however, were unique to the EPIC array, which suggests that we captured additional meaningful associations that were not included in the meta-analysis for this chemical. Since the lambda was slightly inflated for the PFOS analysis, results should be interpreted with caution.

Our results build from previous epidemiological studies including one to two cohorts each that show associations between prenatal PFAS exposures with offspring DNAm assessed via similar methods. As summarized in a previous review, PFHxS, PFOA, PFOS, PFDA, and PFNA have been studied in epigenome-wide association studies, and associations between each of these PFAS and DNAm have been identified. However, the sites identified in the present study did not overlap with those previously identified [34, 38]. While not the exact same CpG sites or regions, loci within the genes *PTCH1, SLC6A2, CCDC40*, and *ZDHHC14* were identified in our study and also as associated with PFNA when including longitudinal measures of DNAm (cord blood and in blood collected at 12 years of age) from the HOME study [36].

Collectively, the ECHO analysis and past studies suggest that prenatal exposures to various PFAS have the potential to modify DNAm at a modest number of loci. Our analysis contributes evidence for PFOA, PFOS, PFHxS, and PFNA. PFAS exposure range or dose in various cohorts may influence the ability to detect differential methylation. The HOME cohort was recruited in the early 2000s and median PFNA levels higher—equivalent to or higher than the 75th percentiles for each ECHO cohort included here [36]. PFOS, PFOA, and PFHxS concentrations varied widely in the ECHO cohort with the oldest cohort having the highest levels (Project Viva), as expected. Previous studies of prenatal PFAS exposure and newborn DNAm that reported notable associations for these PFAS had medians and ranges of exposure that were within the levels observed in the ECHO cohorts included here [23, 35, 36, 38, 59]. While no associations were observed with PFDA, serum concentrations in the ECHO cohorts were low (medians <0.4 ng/mL), and it is unknown whether higher exposures to PFDA may alter the newborn epigenome.

PFOA was inversely associated with DNAm at a region of three consecutive sites annotated to the gene *SSR3*. This DMR is located in a south shore relative to a CpG island. *SSR3* is a translocation-associated protein complex that has known roles in various diseases including cancers. Specifically, this gene functions to facilitate the translocation of polypeptides across the membrane of the endoplasmic reticulum [60]. PFHxS exposure was positively associated with methylation in a site within an exon of the *CASC3* gene, and this association was also significant in MMIP but in the opposite direction. CASC3 is a component of the spliceosome that is required for pre-mRNA splicing. As a core component of the exon junction complex, CASC3 promotes transcriptome-wide activation of nonsense-mediated decay, an mRNA quality control mechanism [61]. Decreased placental expression of *CASC3* was previously reported in a murine study of prenatal PFHxS exposure [62]. PFOS exposure was associated with six CpG sites in our meta-analysis including both the 450K and EPIC arrays. From this analysis, we identified associations between PFOS exposure and methylation changes at the leptin (*LEP*) gene. *LEP* is important for regulating energy homeostasis, adipogenesis, and food intake [63]. Higher circulating levels of leptin have been identified in individuals with obesity [63]. Interestingly, exposure to PFAS, including PFOS specifically, has been associated with obesity risk among individuals [64]. Therefore, it would be important to consider whether methylation changes at *LEP* impact gene expression and whether this serves as a mediator between PFAS exposure and weight regulation. According to the Comparative Toxicogenomics Database, altered expression of several of the differentially methylated genes—*ABR, LEP, SERPINA1*, and *LOXL1*—have been associated with PFHxS, PFOA, and/or PFOS in various animal models of exposure, suggesting that, along with *CASC3*, these may be PFAS-responsive genes whose involvement in PFAS toxicity should be evaluated further. Seven sites from the EPIC-only analysis replicated in MMIP (in intergenic regions or *FGGY, ODZ4, SLC47A1, WDFY3*, and *TMEM131*). *FGGY, SLC47A1*, and *TMEM31* expression were altered by PFAS exposure in past cell or animal exposure models [65–67], and these may be PFAS responsive genes for consideration in future studies.

There are several mechanisms by which PFAS exposure could disrupt the establishment of DNAm patterns in early development or their maintenance. One potential mechanism is through disruption of peroxisome proliferator-activated receptor (PPAR) activity. Many PFAS are known to bind to and either activate or disrupt the transcription factor PPAR-alpha (PPARA) activity and in some cases other PPARs [55–58]. For example, seven of eight tested PFAS activated PPARA *in vitro* [58]. Transcription factor occupancy is one mechanism by which exposures lead to gene-specific epigenetic changes [68, 69]. Activation of PPARA or other transcription

**Table 5.** Statistically significant associations between PFAS and DNAm from the EPIC-only analysis ($q$-value < 0.05)

| PFAS | Gene name | Probe ID | Genomic location** | Relation to CpG island | Effect estimate | Standard error | P-value | FDR ($q$-value) | Direction** | Heterogeneity $I^2$ | Heterogeneity P-value |
|---|---|---|---|---|---|---|---|---|---|---|---|
| PFNA | | cg13617714* | chr6:159 363 639 | S. Shelf | 0.0305 | 0.0054 | 1.96E−08 | 0.014 | ++ | 39 | 0.20 |
| PFOA | | cg01301339 | chr5:180 673 096 | Island | 0.0104 | 0.0019 | 4.48E−08 | 0.030 | ++ | 0 | 0.89 |
| PFOS | | cg03022395* | chr20:57 940 960 | Open Sea | 0.0187 | 0.0029 | 1.18E−10 | 8.69E−05 | ++ | 92.3 | 3.02E−04 |
| PFOS | | cg01855290* | chr21:45 132 261 | Open Sea | 0.0074 | 0.0013 | 4.25E−09 | 0.002 | +− | 78 | 0.03 |
| PFOS | *GPS1* | cg17616192* | chr17:80 009 015 | Island | 0.016 | 0.0028 | 8.97E−09 | 0.002 | ++ | 0 | 0.90 |
| PFOS | | cg16814322* | chr14:101 281 050 | Open Sea | 0.0118 | 0.0021 | 2.54E−08 | 0.004 | ++ | 0 | 0.47 |
| PFOS | *ZNF354A* | cg20410135 | chr5:178 157 962 | S. Shore | −0.0113 | 0.002 | 2.70E−08 | 0.004 | −+ | 80.1 | 0.03 |
| PFOS | | cg11678328* | chr5:151 082 728 | Open Sea | 0.0054 | 0.001 | 3.69E−08 | 0.005 | +− | 87 | 0.01 |
| PFOS | *PLA2G4F* | cg22490420* | chr15:42 434 040 | Open Sea | 0.0118 | 0.0022 | 5.77E−08 | 0.006 | ++ | 74.7 | 0.05 |
| PFOS | | cg21536734* | chr5:35 355 272 | Open Sea | 0.0073 | 0.0014 | 8.73E−08 | 0.008 | ++ | 0 | 0.83 |
| PFOS | *PTCH1* | cg17647195* | chr9:98 213 015 | Open Sea | 0.0047 | 9.00E−04 | 1.18E−07 | 0.009 | ++ | 0 | 0.84 |
| PFOS | | cg18750782* | chr10:102 374 055 | Open Sea | 0.0087 | 0.0017 | 1.17E−07 | 0.009 | ++ | 0 | 0.48 |
| PFOS | | cg07905372* | chr19:31 757 966 | Open Sea | 0.0074 | 0.0014 | 1.35E−07 | 0.009 | ++ | 39.2 | 0.20 |
| PFOS | | cg01624707* | chr5:157 966 020 | Open Sea | 0.0151 | 0.0029 | 2.19E−07 | 0.010 | ++ | 63.9 | 0.10 |
| PFOS | *COL6A3* | cg05223158* | chr2:238 271 966 | Open Sea | 0.0075 | 0.0014 | 1.98E−07 | 0.010 | ++ | 0 | 0.53 |
| PFOS | *UBE2QL1* | cg15791160* | chr5:6 494 429 | Open Sea | 0.0085 | 0.0016 | 2.40E−07 | 0.010 | ++ | 0 | 0.43 |
| PFOS | *LINC00659* | cg22108823* | chr20:61 406 786 | S. Shelf | 0.0105 | 0.002 | 2.07E−07 | 0.010 | ++ | 85.4 | 0.01 |
| PFOS | | cg25963609* | chr15:77 390 691 | Open Sea | 0.0087 | 0.0017 | 1.90E−07 | 0.010 | ++ | 0 | 0.83 |
| PFOS | | cg26046406* | chr22:44 780 198 | Open Sea | 0.0137 | 0.0026 | 2.32E−07 | 0.010 | ++ | 0 | 0.51 |
| PFOS | *TMCO4* | cg00576736 | chr1:20 030 383 | Open Sea | 0.0049 | 0.001 | 3.35E−07 | 0.014 | +- | 73.4 | 0.05 |
| PFOS | *ADORA2A* | cg22209520* | chr22:24 819 482 | N. Shore | 0.0082 | 0.0016 | 3.54E−07 | 0.014 | ++ | 0 | 0.67 |
| PFOS | | cg10024209* | chr7:101 204 266 | Open Sea | 0.007 | 0.0014 | 4.30E−07 | 0.014 | ++ | 0 | 0.50 |
| PFOS | *NCBP1* | cg17850275* | chr9:100 427 644 | Open Sea | 0.0055 | 0.0011 | 4.01E−07 | 0.014 | ++ | 0 | 0.93 |
| PFOS | *CDH4* | cg18998003 | chr20:60 388 715 | Open Sea | 0.0049 | 0.001 | 4.19E−07 | 0.014 | ++ | 0 | 0.65 |
| PFOS | | cg22039336* | chr10:132 877 666 | S. Shelf | 0.0083 | 0.0017 | 4.63E−07 | 0.015 | ++ | 0 | 0.40 |
| PFOS | *DUSP27* | cg13179074 | chr1:167 064 091 | Open Sea | 0.0069 | 0.0014 | 5.73E−07 | 0.017 | ++ | 22.5 | 0.26 |
| PFOS | *SLC6A2* | cg16338844* | chr16:55 738 066 | Open Sea | 0.0113 | 0.0023 | 5.52E−07 | 0.017 | ++ | 0 | 0.62 |
| PFOS | | cg10626792 | chr11:1 849 375 | S. Shore | 0.0065 | 0.0013 | 5.99E−07 | 0.017 | ++ | 0 | 0.99 |
| PFOS | | cg25107667* | chr20:51 042 037 | Open Sea | 0.0161 | 0.0032 | 6.41E−07 | 0.017 | +− | 68.5 | 0.07 |
| PFOS | *TBXAS1* | cg04765497* | chr7:139 700 814 | Open Sea | 0.006 | 0.0012 | 8.28E−07 | 0.022 | ++ | 0 | 0.39 |
| PFOS | *INADL* | cg12213182* | chr1:62 547 123 | Open Sea | 0.0063 | 0.0013 | 8.76E−07 | 0.022 | ++ | 39.9 | 0.20 |
| PFOS | *EBF3* | cg00185660 | chr10:131 667 994 | S. Shore | 0.0047 | 0.001 | 1.10E−06 | 0.025 | ++ | 0 | 0.89 |
| PFOS | *CABLES2* | cg03801680* | chr20:60 977 964 | Open Sea | 0.0117 | 0.0024 | 1.05E−06 | 0.025 | ++ | 90.4 | 0.00 |
| PFOS | *MVD* | cg04044356* | chr16:88 721 965 | Island | 0.0114 | 0.0024 | 1.19E−06 | 0.025 | ++ | 45.3 | 0.18 |
| PFOS | *RORC* | cg14567142* | chr1:151 779 765 | Open Sea | 0.008 | 0.0016 | 1.19E−06 | 0.025 | ++ | 0 | 0.41 |
| PFOS | *FGGY* | cg15591629* | chr1:60 018 296 | Open Sea | 0.0058 | 0.0012 | 1.11E−06 | 0.025 | ++ | 0 | 0.61 |
| PFOS | | cg23672990* | chr18:45 918 338 | Open Sea | 0.0061 | 0.0013 | 1.15E−06 | 0.025 | ++ | 71.3 | 0.06 |
| PFOS | *ODZ4* | cg03825175 | chr11:78 780 248 | N. Shore | 0.006 | 0.0012 | 1.23E−06 | 0.025 | ++ | 72.7 | 0.06 |
| PFOS | *GAK* | cg26116732* | chr4:876 727 | Island | 0.0117 | 0.0024 | 1.43E−06 | 0.028 | ++ | 70.2 | 0.07 |
| PFOS | *NEDD9* | cg15755230* | chr6:11 190 956 | Open Sea | 0.0119 | 0.0025 | 1.52E−06 | 0.029 | ++ | 76 | 0.04 |
| PFOS | *ARHGAP42* | cg00858941* | chr11:100 702 777 | Open Sea | 0.0222 | 0.0046 | 1.63E−06 | 0.030 | ++ | 0 | 0.44 |
| PFOS | *GAL3ST3* | cg16325573* | chr11:65 813 492 | N. Shelf | 0.0055 | 0.0011 | 1.62E−06 | 0.030 | ++ | 0 | 0.69 |
| PFOS | | cg04782589* | chr9:134 720 175 | S. Shelf | 0.0066 | 0.0014 | 1.70E−06 | 0.030 | ++ | 0 | 0.62 |
| PFOS | | cg12024316* | chr1:153 481 914 | Open Sea | 0.0084 | 0.0017 | 1.72E−06 | 0.030 | ++ | 0 | 0.59 |
| PFOS | | cg00875849* | chr10:118 569 527 | Open Sea | 0.0143 | 0.003 | 1.91E−06 | 0.033 | ++ | 0 | 0.78 |

(continued)

**Table 5.** (Continued)

| PFAS | Gene name | Probe ID | Genomic location** | Relation to CpG island | Effect estimate | Standard error | P-value | FDR (*q*-value) | Direction** | Heterogeneity $I^2$ | Heterogeneity *P*-value |
|---|---|---|---|---|---|---|---|---|---|---|---|
| PFOS | *TMEM72-AS1* | cg12080553* | chr10:45 315 980 | Open Sea | 0.0116 | 0.0024 | 1.95E−06 | 0.033 | ++ | 75.8 | 0.04 |
| PFOS | *BLCAP* | cg03226872 | chr20:36 153 865 | N. Shelf | 0.0062 | 0.0013 | 2.20E−06 | 0.033 | ++ | 0 | 0.42 |
| PFOS | *C6orf195* | cg05802990* | chr6:2 636 796 | S. Shore | 0.0085 | 0.0018 | 2.13E−06 | 0.033 | ++ | 54.8 | 0.14 |
| PFOS | *SLC47A1* | cg05947984* | chr17:19 470 287 | Open Sea | 0.0072 | 0.0015 | 2.18E−06 | 0.033 | ++ | 53.7 | 0.14 |
| PFOS | | cg14250330* | chr9:38 734 797 | Open Sea | 0.0064 | 0.0014 | 2.22E−06 | 0.033 | ++ | 1.6 | 0.31 |
| PFOS | *ARMC9* | cg21015554* | chr2:232 062 665 | N. Shore | 0.0095 | 0.002 | 2.21E−06 | 0.033 | +− | 78.7 | 0.03 |
| PFOS | *KCTD21-AS1* | cg25864358* | chr11:77 878 003 | Open Sea | 0.0062 | 0.0013 | 2.24E−06 | 0.033 | ++ | 9.9 | 0.29 |
| PFOS | *RASSF2* | cg12322852 | chr20:4 764 077 | Open Sea | 0.0064 | 0.0014 | 2.30E−06 | 0.033 | +− | 85.4 | 0.01 |
| PFOS | *C12orf57* | cg09901208 | chr12:7 052 614 | N. Shore | 0.0047 | 0.001 | 2.45E−06 | 0.034 | ++ | 0 | 0.76 |
| PFOS | *KRT79* | cg11934394* | chr12:53 215 390 | Open Sea | 0.009 | 0.0019 | 2.48E−06 | 0.034 | ++ | 0 | 0.64 |
| PFOS | *SH2B2* | cg09223851 | chr7:101 938 115 | S. Shore | 0.007 | 0.0015 | 2.58E−06 | 0.034 | ++ | 39.4 | 0.20 |
| PFOS | | cg21050416 | chr5:159 411 100 | N. Shelf | 0.006 | 0.0013 | 2.56E−06 | 0.034 | +− | 81.2 | 0.02 |
| PFOS | | cg02116058* | chr3:133 971 155 | S. Shore | 0.0065 | 0.0014 | 2.70E−06 | 0.035 | +− | 91.8 | 0.00 |
| PFOS | | cg23782909* | chr12:101 945 864 | Open Sea | 0.0095 | 0.002 | 2.69E−06 | 0.035 | ++ | 62.1 | 0.10 |
| PFOS | *CES8* | cg02578103* | chr16:67 021 154 | Open Sea | 0.0078 | 0.0017 | 2.84E−06 | 0.035 | ++ | 0 | 0.80 |
| PFOS | | cg15920561 | chr14:73 083 724 | Open Sea | 0.0057 | 0.0012 | 2.83E−06 | 0.035 | ++ | 0 | 0.62 |
| PFOS | | cg05195452 | chr15:93 126 847 | Open Sea | 0.0054 | 0.0012 | 3.06E−06 | 0.036 | ++ | 80 | 0.03 |
| PFOS | *ABLIM2* | cg06489182* | chr4:8 119 983 | Open Sea | 0.0064 | 0.0014 | 2.99E−06 | 0.036 | ++ | 0 | 0.64 |
| PFOS | | cg18000295* | chr1:231 031 988 | Open Sea | 0.0076 | 0.0016 | 2.92E−06 | 0.036 | ++ | 0 | 0.39 |
| PFOS | *NHEJ1* | cg23220105* | chr2:219 990 589 | Open Sea | 0.0125 | 0.0027 | 3.01E−06 | 0.036 | ++ | 0 | 0.73 |
| PFOS | *QTRT1* | cg00658836* | chr19:10 818 034 | Open Sea | 0.0042 | 9.00E−04 | 3.99E−06 | 0.036 | ++ | 0 | 0.40 |
| PFOS | *EIF2S2* | cg01562356* | chr20:32 701 112 | S. Shore | 0.0076 | 0.0016 | 3.39E−06 | 0.036 | ++ | 0 | 0.44 |
| PFOS | | cg02265758* | chr5:767 440 | Open Sea | 0.0155 | 0.0033 | 3.49E−06 | 0.036 | ++ | 16.5 | 0.27 |
| PFOS | *STK33* | cg03169390* | chr11:8 606 180 | Open Sea | 0.0067 | 0.0014 | 3.39E−06 | 0.036 | ++ | 0 | 0.65 |
| PFOS | *WDFY3* | cg04355093* | chr4:85 887 382 | Island | 0.0092 | 0.002 | 4.06E−06 | 0.036 | ++ | 82.1 | 0.02 |
| PFOS | *TBC1D1* | cg05158273* | chr4:37 928 104 | Open Sea | 0.0048 | 0.001 | 3.62E−06 | 0.036 | +− | 76.9 | 0.04 |
| PFOS | | cg07271512* | chr16:89 146 121 | N. Shore | 0.0077 | 0.0017 | 3.64E−06 | 0.036 | ++ | 0 | 0.41 |
| PFOS | *KALRN* | cg08383262* | chr3:123 987 194 | N. Shore | 0.0088 | 0.0019 | 3.46E−06 | 0.036 | +− | 67.7 | 0.08 |
| PFOS | *PLXNC1* | cg09366587* | chr12:94 559 051 | Open Sea | 0.0253 | 0.0055 | 3.87E−06 | 0.036 | ++ | 87.9 | 0.00 |
| PFOS | *LINC00595* | cg10972184* | chr10:80 026 812 | Open Sea | 0.007 | 0.0015 | 4.01E−06 | 0.036 | ++ | 0 | 0.82 |
| PFOS | *PDGFRL* | cg12063034* | chr8:17 489 487 | Open Sea | 0.014 | 0.003 | 3.97E−06 | 0.036 | ++ | 76.2 | 0.04 |
| PFOS | *STK35* | cg12362077* | chr20:2 081 907 | N. Shore | 0.0099 | 0.0021 | 3.72E−06 | 0.036 | ++ | 0 | 0.85 |
| PFOS | *LFNG* | cg14602936* | chr7:2 558 096 | N. Shore | 0.0041 | 9.00E−04 | 3.73E−06 | 0.036 | ++ | 0 | 0.32 |
| PFOS | | cg14789175* | chr1:11 534 690 | N. Shelf | 0.0083 | 0.0018 | 3.71E−06 | 0.036 | +− | 85 | 0.01 |
| PFOS | | cg15508544* | chr1:53 966 613 | Open Sea | 0.0072 | 0.0015 | 3.79E−06 | 0.036 | ++ | 0 | 0.95 |
| PFOS | *TMEM131* | cg17238473* | chr2:98 378 600 | Open Sea | 0.0047 | 0.001 | 3.47E−06 | 0.036 | ++ | 56.2 | 0.13 |
| PFOS | | cg17519955* | chr1:184 634 036 | S. Shore | 0.0076 | 0.0016 | 3.59E−06 | 0.036 | ++ | 0 | 0.51 |
| PFOS | *TRIM62* | cg23015434* | chr1:33 635 479 | Open Sea | 0.0068 | 0.0015 | 4.12E−06 | 0.036 | ++ | 18.3 | 0.27 |
| PFOS | *CTIF* | cg25050105* | chr18:46 356 097 | Open Sea | 0.0037 | 8.00E−04 | 3.90E−06 | 0.036 | +− | 89.2 | 0.00 |
| PFOS | *PRKAR1B* | cg25402422 | chr7:653 680 | Open Sea | 0.0061 | 0.0013 | 3.45E−06 | 0.036 | ++ | 69.1 | 0.07 |
| PFOS | *IZUMO1* | cg26931208* | chr19:49 244 592 | S. Shore | 0.0201 | 0.0044 | 4.08E−06 | 0.036 | +− | 75.5 | 0.04 |
| PFOS | *EPHB1* | cg10852616* | chr3:134 616 616 | Open Sea | 0.0074 | 0.0016 | 4.41E−06 | 0.037 | ++ | 0 | 0.82 |
| PFOS | *LAMA3* | cg13200691* | chr18:21 518 723 | Open Sea | 0.0051 | 0.0011 | 4.39E−06 | 0.037 | ++ | 36.2 | 0.21 |
| PFOS | *SNTG2* | cg21428070* | chr2:1 350 350 | Open Sea | 0.0075 | 0.0016 | 4.32E−06 | 0.037 | ++ | 0 | 0.54 |
| PFOS | | cg27519282* | chr15:90 313 591 | Open Sea | 0.0089 | 0.0019 | 4.32E−06 | 0.037 | ++ | 0 | 0.61 |

(continued)

**Table 5.** (Continued)

| PFAS | Gene name | Probe ID | Genomic location** | Relation to CpG island | Effect estimate | Standard error | P-value | FDR (q-value) | Direction** | Heterogeneity $I^2$ | Heterogeneity P-value |
|---|---|---|---|---|---|---|---|---|---|---|---|
| PFOS | *SNX19* | cg14779329* | chr11:130 786 720 | S. Shore | 0.016 | 0.0035 | 4.46E–06 | 0.037 | ++ | 0 | 0.84 |
| PFOS | | cg15780653* | chr11:128 486 035 | Open Sea | 0.0096 | 0.0021 | 4.52E–06 | 0.037 | +– | 85.7 | 0.01 |
| PFOS | *ADCY9* | cg09032423* | chr16:4 015 231 | Island | 0.0213 | 0.0046 | 4.60E–06 | 0.037 | ++ | 82.1 | 0.02 |
| PFOS | | cg07101495* | chr2:33 637 091 | Open Sea | 0.0069 | 0.0015 | 5.16E–06 | 0.041 | ++ | 0 | 0.81 |
| PFOS | | cg02412616 | chr22:46 422 752 | N. Shore | 0.0059 | 0.0013 | 5.57E–06 | 0.041 | ++ | 0 | 0.86 |
| PFOS | *C2orf81* | cg02466544* | chr2:74 641 453 | N. Shore | 0.0078 | 0.0017 | 5.50E–06 | 0.041 | ++ | 0 | 0.94 |
| PFOS | *LAMB3* | cg03917982* | chr1:209 820 722 | Open Sea | 0.0069 | 0.0015 | 5.35E–06 | 0.041 | ++ | 59.6 | 0.12 |
| PFOS | *ANKRD55* | cg15431103* | chr5:55 457 410 | Open Sea | –0.0104 | 0.0023 | 5.57E–06 | 0.041 | –+ | 37.3 | 0.21 |
| PFOS | | cg17063632* | chr6:43 989 118 | Open Sea | 0.0078 | 0.0017 | 5.36E–06 | 0.041 | ++ | 0 | 0.42 |
| PFOS | *MADD* | cg18277168* | chr11:47 294 832 | S. Shelf | 0.0042 | 9.00E–04 | 5.58E–06 | 0.041 | ++ | 0 | 0.48 |
| PFOS | *ITPR3* | cg24909371* | chr6:33 627 751 | Open Sea | 0.0058 | 0.0013 | 5.40E–06 | 0.041 | ++ | 0 | 0.63 |
| PFOS | *DPP6* | cg13016237 | chr7:154 681 513 | N. Shelf | 0.0066 | 0.0014 | 5.72E–06 | 0.042 | ++ | 0 | 0.83 |
| PFOS | *WSCD1* | cg15690190* | chr17:5 984 640 | Open Sea | 0.0083 | 0.0018 | 5.68E–06 | 0.042 | ++ | 87.1 | 0.01 |
| PFOS | | cg21610838* | chr16:58 698 889 | Open Sea | 0.0059 | 0.0013 | 5.83E–06 | 0.042 | ++ | 0 | 0.56 |
| PFOS | *SLC34A1* | cg25851453* | chr5:176 815 647 | Open Sea | 0.006 | 0.0013 | 5.82E–06 | 0.042 | ++ | 0 | 0.70 |
| PFOS | *PALM2* | cg14105456* | chr9:112 688 699 | Open Sea | 0.0059 | 0.0013 | 5.91E–06 | 0.042 | ++ | 0 | 0.57 |
| PFOS | *LOC100132354* | cg01172073 | chr6:43 857 911 | Open Sea | 0.0056 | 0.0012 | 6.01E–06 | 0.042 | ++ | 0 | 0.51 |
| PFOS | | cg08353973 | chr15:66 914 175 | N. Shore | 0.0064 | 0.0014 | 6.22E–06 | 0.043 | ++ | 0 | 0.66 |
| PFOS | *LINC00700* | cg10264044* | chr10:2 054 055 | Open Sea | 0.0089 | 0.002 | 6.24E–06 | 0.043 | ++ | 0 | 0.35 |
| PFOS | *RGS3* | cg18426557* | chr9:116 346 602 | Island | 0.0142 | 0.0031 | 6.34E–06 | 0.043 | ++ | 0 | 0.81 |
| PFOS | | cg18749309* | chr11:61 434 800 | Open Sea | 0.0095 | 0.0021 | 6.29E–06 | 0.043 | +– | 89.3 | 0.00 |
| PFOS | *BDKRB1* | cg02319068* | chr14:96 728 517 | Open Sea | 0.0064 | 0.0014 | 6.46E–06 | 0.043 | ++ | 0 | 0.73 |
| PFOS | *MED15* | cg20633070* | chr22:20 931 299 | Open Sea | 0.0055 | 0.0012 | 6.51E–06 | 0.043 | ++ | 64.5 | 0.09 |
| PFOS | *LOC441204* | cg09510757* | chr7:26 492 211 | Open Sea | 0.0083 | 0.0018 | 6.90E–06 | 0.044 | ++ | 0 | 0.37 |
| PFOS | | cg11401165* | chr8:62 722 700 | Open Sea | 0.0033 | 7.00E–04 | 6.84E–06 | 0.044 | ++ | 0 | 0.67 |
| PFOS | | cg22036605 | chr2:241 587 783 | S. Shore | 0.0055 | 0.0012 | 6.78E–06 | 0.044 | ++ | 0 | 0.34 |
| PFOS | *SNAP47* | cg04279396* | chr1:227 932 553 | Open Sea | 0.0058 | 0.0013 | 7.28E–06 | 0.045 | ++ | 65.2 | 0.09 |
| PFOS | | cg09894814 | chr1:222 217 065 | Open Sea | 0.0056 | 0.0012 | 7.22E–06 | 0.045 | ++ | 0 | 0.91 |
| PFOS | *DOCK9* | cg18916584* | chr13:99 492 834 | Open Sea | 0.0096 | 0.0021 | 7.33E–06 | 0.045 | ++ | 0 | 0.53 |
| PFOS | *NME5* | cg20321998* | chr5:137 476 346 | Open Sea | 0.0061 | 0.0013 | 7.28E–06 | 0.045 | ++ | 0 | 0.56 |
| PFOS | *PPARGC1A* | cg27365602* | chr4:23 890 206 | Open Sea | 0.0046 | 0.001 | 7.09E–06 | 0.045 | ++ | 15 | 0.28 |
| PFOS | *FAM170B* | cg27406618 | chr10:50 341 989 | S. Shore | 0.0064 | 0.0014 | 7.53E–06 | 0.046 | ++ | 0 | 0.56 |
| PFOS | | cg01219495* | chr11:71 288 546 | S. Shore | 0.0041 | 9.00E–04 | 7.70E–06 | 0.047 | ++ | 0 | 0.36 |
| PFOS | *CCDC40* | cg19592176 | chr17:78 039 096 | N. Shore | 0.0043 | 0.001 | 7.77E–06 | 0.047 | ++ | 0 | 0.65 |
| PFOS | *NBAS* | cg18451529* | chr2:15 698 011 | N. Shelf | 0.0092 | 0.0021 | 7.85E–06 | 0.047 | +– | 77.7 | 0.03 |
| PFOS | *FGFR1* | cg14733725* | chr8:38 315 580 | Open Sea | 0.0153 | 0.0034 | 7.92E–06 | 0.047 | ++ | 62.9 | 0.10 |
| PFOS | | cg01283167* | chr11:69 605 773 | Open Sea | 0.0114 | 0.0026 | 8.04E–06 | 0.047 | ++ | 64 | 0.10 |
| PFOS | | cg04503063* | chr1:150 282 391 | Open Sea | 0.0072 | 0.0016 | 8.10E–06 | 0.047 | ++ | 0 | 0.81 |
| PFOS | | cg08043781 | chr2:62 568 338 | Open Sea | 0.0037 | 8.00E–04 | 8.21E–06 | 0.047 | ++ | 0 | 0.63 |
| PFOS | *NCOR2* | cg22863744 | chr12:124 942 176 | S. Shore | –0.0029 | 7.00E–04 | 8.17E–06 | 0.047 | –+ | 81 | 0.02 |
| PFOS | *IGFALS* | cg00629117 | chr16:1 844 932 | S. Shelf | 0.0056 | 0.0013 | 8.39E–06 | 0.048 | ++ | 0 | 0.72 |
| PFOS | *CREB3L1* | cg09709565* | chr11:46 316 283 | N. Shore | 0.0077 | 0.0017 | 8.76E–06 | 0.049 | ++ | 0 | 0.72 |
| PFOS | *KIF2B* | cg13521991* | chr17:51 900 096 | Open Sea | 0.0083 | 0.0019 | 8.80E–06 | 0.049 | ++ | 0 | 0.70 |
| PFOS | *IKBKE* | cg02830006* | chr1:206 649 727 | Open Sea | 0.0094 | 0.0021 | 8.95E–06 | 0.049 | +– | 91.9 | 0.00 |
| PFOS | | cg17239714* | chr8:127 546 956 | Open Sea | 0.0043 | 0.001 | 8.95E–06 | 0.049 | ++ | 0 | 1.00 |

*Unique to EPIC array, not included in the 450K array, and thus excluded from the meta-analysis.
**Locations are according to genome build GRCh37/hg19.
The 'direction' column refers to concordance in the direction of effect across the meta-analysed datasets.

factors by PFAS during early gestation could lead to aberrant binding of PPARA to its target genes, thereby altering recruitment of the machinery needed for epigenetic reprogramming (i.e. inhibiting DNA methyltransferase binding). Changes in the DNAm profile would then be propagated following mitosis. Among the genes we identified with CpG sites or regions associated with any PFAS, we identified a number of PPAR target genes from various publicly available databases [55, 70, 71]. Specifically, from our EPIC-only analysis, 30/133 genes associated with prenatal PFOS exposure were predicted to be PPAR gamma target genes, and 22/133 genes were predicted to be PPAR delta target genes [70, 71]. Of these genes, a number are predicted or verified to be targeted by both PPAR gamma and delta including *PPARGC1A*, which is verified to be upregulated by both [55, 70, 71], *NCOR2, FGGY, TBXAS1, CREB3L1, NEDD9, NBAS*, and *FGFR1*. In our total meta-analysis, of the six CpG sites associated with PFOS exposure prenatally, *ABR* is predicted to be a target of PPAR delta, while *LEP* is predicted to be a target of PPAR gamma [70, 71]. This particular finding further supports future investigation into the role of methylation at *LEP* as a mediator of the impact of PFAS on adiposity-related outcomes, as both *LEP* and PPAR gamma, independently, and in concert with one another, are involved in the development and function of adipocytes, and their dysregulation has been associated with obesity [63, 72, 73]. *SSR3*, which was annotated to a DMR associated with prenatal PFOA exposure, is predicted to be a target of both PPAR gamma and delta.

PFAS may influence both DNAm and DNA hydroxymethylation through altered regulation of DNAm machinery. For example, a mouse study demonstrated decreased expression of *Dnmt3a*, which encodes the enzyme responsible for de novo methylation, increased expression of the maintenance methylator *Dnmt1*, and decreased expression of *Tet1* (responsible for oxidation of methylation to hydroxymethylation) in kidney following PFOA exposure, correlating with DNAm changes at 879 genes [74]. In human hepatocytes, PFOA decreased expression of *TET1*, while the replacement PFAS, GenX, decreased expression of *DNMT1, DNMT3b*, and *DNMT3a* [75]. In our past MMIP study that estimated 5-methylcytosine and 5-hydroxymethylcytosine levels separately in cord blood DNA, we discovered hundreds to thousands of loci with altered levels of either or both of these marks [38]. Thus, we may have identified more associations with PFAS in the current study if data on the individual modifications were available instead of the more commonly measured total DNAm. PFAS exposures also lead to oxidative stress, which can indirectly impact DNAm maintenance pathways; PFOS exposure during pregnancy in particular has been linked to increased oxidative stress biomarkers [76, 77].

A major strength of this study is the use of pooled data from six cohorts within the ECHO Cohort that represent diverse racial, ethnic and socioeconomic backgrounds in the USA and have a wide range of PFAS exposure levels. The focus on five PFAS—including PFDA, which has not been included in most epigenomic analyses in the past—is also a strength. Utilizing total DNAm data from the 450K and EPIC arrays is a strength because it allows us to build on research by others. However, there is evidence that PFAS may influence 5-hydroxymethylcytosine and 5-methylcytosine separately, and we were not able to capture these nuances with total methylation data [38]. We also did not measure other modifications beyond DNAm that are important for epigenetic programming. To avoid issues with differences in the 450K and EPIC arrays, we conducted a meta-analysis of common probes across both arrays after running analyses in the 450K and EPIC datasets separately. Even with more than 1000 participants, our sample was not powered for stratified analyses by sex, race, and ethnicity, or other potential modifiers. Additionally, we had limited sample size for our EPIC-only analyses, so these results should be interpreted with caution. While we used FDR to reduce the number of false positives, if we had used the stringent Bonferroni correction, one CpG site in the main analysis remains statistically significant (the association between PFOS and cg06528150 in *KIAA1841*). PFAS were measured at different time points across pregnancy in the cohorts, and we only had a single PFAS measure for each participant. Thus, we captured a snapshot in time of an individual's exposure and related this to an epigenetic outcome also at a single timepoint—birth. Therefore, it is possible that over long periods of time, the relationship between PFAS exposure and DNAm (such as in childhood or adolescence) may change. With regard to having a single exposure, however, most of the PFAS measured have long half-lives (up to years). Thus, measurement at any time point during pregnancy reflects the general exposure level of the foetus throughout pregnancy [13].

## Conclusion

This study is the first multicohort analysis of prenatal PFAS exposure and newborn blood DNAm. Our results build upon previous cohort studies and provide further evidence to support that PFOA, PFOS, PFHxS, and PFNA exposures in pregnancy are associated with offspring DNA methylome in a diverse population from the USA. This information furthers our understanding of how the epigenome might mediate the effects of prenatal PFAS exposure on child health outcomes, an area of intense interest. It also serves to contribute data to the environmental and human health risk assessment of PFAS, as the regulatory framework around this class of chemicals is an important public health issue, particularly as it relates to exposures during pregnancy. DNAm changes identified at birth have the broad potential to be developed and validated to serve as a biomarker of past exposure, illuminate mechanistic links between exposure and disease, and inform therapeutic targets to disrupt exposure-associated toxicity to improve health outcomes. Strengthening our understanding of the relationship between prenatal PFAS exposure and the epigenome at birth will facilitate the development of these biomarkers and therapeutic targets, with the common goal of alleviating the burden of these exposures on children's health.

## Acknowledgements

The authors wish to thank our ECHO Colleagues; the medical, nursing, and program staff; and the children and families participating in the ECHO cohort.

## Supplementary data

Supplementary data is available at *EnvEpig* online.

Conflict of interest. None declared.

## Funding

Research reported in this publication was supported by the Environmental influences on Child Health Outcomes (ECHO) program, Office of the Director, National Institutes of Health, under Award Numbers U2COD023375 (Coordinating Center), U24OD023382 (Data Analysis Center), U24OD023319 with co-funding from the Office of Behavioral and Social Science Research (Measurement Core), U24OD035523 (Lab Core), ES0266542 (HHEAR), U24ES026539 (HHEAR Barbara O'Brien), U2CES026533 (HHEAR Lisa Peter

son), U2CES026542 (HHEAR Patrick Parsons, Kannan Kurunthacalam), U2CES030859 (HHEAR Manish Arora), U2CES030857 (HHEAR Timothy R. Fennell, Susan J. Sumner, Xiuxia Du), U2CES026555 (HHEAR Susan L. Teitelbaum), U2CES026561 (HHEAR Robert O. Wright), U2CES030851 (HHEAR Heather M. Stapleton, P. Lee Fergus on), UG3/UH3OD023251 (Akram Alshawabkeh), UH3OD023320 and UG3OD035546 (Judy Aschner), UH3OD023332 (Clancy Blair, Leonardo Trasande), UG3/UH3OD023253 (Carlos Camargo), UG3/UH3OD023248 and UG3OD035526 (Dana Dabelea), UG3/UH3OD023313 (Daphne Koinis Mitchell), UH3OD023328 (Cristiane Duarte), UH3OD023318 (Anne Dunlop), UG3/UH3OD023279 (Amy Elliott), UG3/UH3OD023289 (Assiamira Ferrara), UG3/UH3OD023282 (James Germ), UH3OD023287 (Carrie Breton), UG3/UH3OD023365 (Irva Hertz-Picciotto), UG3/UH3OD023244 (Alison Hipwell), UG3/UH3OD023275 (Margaret Karagas), UH3OD023271 and UG3OD035528 (Catherine Karr), UH3OD023347 (Barry Lester), UG3/UH3OD023389 (Leslie Leve), UG3/UH3OD023344 (Debra MacKenzie), UH3OD023268 (Scott Weiss), UG3/UH3OD023288 (Cynthia McEvoy), UG3/UH3OD023342 (Kristen Lyall), UG3/UH3OD023349 (Thomas O'Connor), UH3OD023286 and UG3OD035533 (Emily Oken), UG3/UH3OD023348 (Mike O'Shea), UG3/UH3OD023285 (Jean Kerver), UG3/UH3OD023290 (Julie Herbstman), UG3/UH3OD023272 (Susan Schantz), UG3/UH3OD023249 (Joseph Stanford), UG3/UH3OD023305 (Leonardo Trasande), UG3/UH3OD023337 (Rosalind Wright), UG3OD035508 (Sheela Sathyanarayana), UG3OD035509 (Anne Marie Singh), UG3OD035513 and UG3OD035532 (Annemarie Stroustrup), UG3OD035516 and UG3OD035517 (Tina Hartert), UG3OD035518 (Jennifer Straughen), UG3OD035519 (Qi Zhao), UG3OD035521 (Katherine Rivera-Spoljaric), UG3OD035527 (Emily S Barrett), UG3OD035540 (Monique Marie Hedderson), UG3OD035543 (Kelly J Hunt), UG3OD035537 (Sunni L Mumford), UG3OD035529 (Hong-Ngoc Nguyen), UG3OD035542 (Hudson Santos), UG3OD035550 (Rebecca Schmidt), UG3OD035536 (Jonathan Slaughter), and UG3OD035544 (Kristina Whitworth).

For the MMIP cohort, funding was provided by NIH grants (R01ES017005 (Vasantha Padmanabhan), P01ES022844 (Padmanabhan), P30ES017885 (Dana Dolinoy), R35ES031686 (Dolinoy), U2CES026553 (Meeker), and the US Environmental Protection Agency (RD83543601, Padmanabhan). Additional funding and laboratory analyses were provided by the National Institute of Environmental Health Sciences Children's Health Exposure Analysis Resource program (U2CES026553).

The content is solely the responsibility of the authors and does not necessarily represent the official views of the National Institutes of Health or the US Environmental Protection Agency.

The sponsor, NIH, participated in the overall design and implementation of the ECHO program, which was funded as a cooperative agreement between NIH and grant awardees. The sponsor approved the Steering Committee-developed ECHO protocol and its amendments including COVID-19 measures. The sponsor had no access to the central database, which was housed at the ECHO Data Analysis Center. Data management and site monitoring were performed by the ECHO Data Analysis Center and Coordinating Center. All analyses for scientific publication were performed by the study statistician, independently of the sponsor. The lead author wrote all drafts of the manuscript and made revisions based on co-authors and the ECHO Publications Committee (a subcommittee of the ECHO Operations Committee) feedback without input from the sponsor. The study sponsor did not review or approve the manuscript for submission to the journal.

## Data availability

Select de-identified data from the ECHO program are available through NICHD's Data and Specimen Hub (DASH). Information on study data not available on DASH can be found on the ECHO study DASH webpage. Data from the MMIP study are available through the National Institutes of Health Human Health Exposure Analysis Resource (NIH HHEAR) data repository (dois: 10.36043/2273_357, 10.36043/2273_358, 10.36043/2273_338, and 10.36043/2273_337). Full results for all CpG sites from meta-analyses are available upon request to the corresponding author.

## Author contributions

Conceived the study: J.M.G. Designed the study: J.M.G., C.L.A., R.S., and V.P. Performed experiments/acquired data: R.S., J.M.G., C.L.A., V.P., D.B.B., C.V.B., A.C., D.D., A.L.D., E.O., A.K.P., D.R., R.J.S., and A.P.S. Analysed data: R.S., J.M.G., and C.L.A. Wrote the paper: R.S. and J.M.G. Edited and approved the manuscript: R.S., C.L.A., V.P., D.B.B., C.V.B., A.C., C.C.C., D.D., A.L.D., M.D.F., M.F.H., E.M.H., A.K.K., E.O., A.K.P., M.C.P., D.R., R.J.S., A.K.S., A.P.S., I.V.Y., Y.Z., and J.M.G.

## References

1. Boronow KE, Brody JG, Schaider LA *et al*. Serum concentrations of PFASs and exposure-related behaviors in African American and non-Hispanic white women. *J Expos Sci Envir Epidemiol* 2019;**29**:206–17.
2. Schaider LA, Balan SA, Blum A *et al*. Fluorinated compounds in U.S. fast food packaging. *Environ Sci Technol Lett* 2017;**4**:105–11.
3. DeLuca NM, Minucci JM, Mullikin A *et al*. Human exposure pathways to poly- and perfluoroalkyl substances (PFAS) from indoor media: a systematic review. *Environ Int* 2022;**162**:107149.
4. Genualdi S, Beekman J, Carlos K *et al*. Analysis of per- and polyfluoroalkyl substances (PFAS) in processed foods from FDA's Total Diet Study. *Anal BioanalChem* 2022;**414**:1189–99.
5. Minet L, Wang Z, Shalin A *et al*. Use and release of per- and polyfluoroalkyl substances (PFASs) in consumer food packaging in U.S. and Canada. *Environ Sci Process Impacts* 2022;**24**:2032–42.
6. Hu XC, Andrews DQ, Lindstrom AB *et al*. Detection of poly- and perfluoroalkyl substances (PFASs) in U.S. drinking water linked to industrial sites, military fire training areas, and wastewater treatment plants. *Environ Sci Technol Lett* 2016;**3**:344–50.
7. Boone JS, Vigo C, Boone T *et al*. Per- and polyfluoroalkyl substances in source and treated drinking waters of the United States. *Sci Total Environ* 2019;**653**:359–69.
8. Andrews D. Report: Up to 110 million Americans could have PFAS-contaminated drinking water. 2018.
9. Smalling KL, Romanok KM, Bradley PM *et al*. Per- and polyfluoroalkyl substances (PFAS) in United States tapwater: comparison of underserved private-well and public-supply exposures and associated health implications. *Environ Int* 2023;**178**:108033.
10. Kidd J, Fabricatore E, Jackson D. Current and future federal and state sampling guidance for per- and polyfluoroalkyl substances in environmental matrices. *Sci Total Environ* 2022;**836**:155523.
11. Langenbach B, and Wilson M. Per- and polyfluoroalkyl substances (PFAS): significance and considerations within the regulatory framework of the USA. *Int J Environ Res Public Health* 2021;**18**: 11142.
12. Sonnenberg NK, Ojewole AE, Ojewole CO *et al*. Trends in serum per- and polyfluoroalkyl substance (PFAS) concentrations in teenagers and adults, 1999–2018 NHANES. *Int J Environ Res Public Health* 2023;**20**:6984.

13. Li Y2, Andersson A, Xu Y *et al*. Determinants of serum half-lives for linear and branched perfluoroalkyl substances after long-term high exposure—a study in Ronneby, Sweden. *Environ Int* 2022;**163**:107198.
14. Nilsson S, Smurthwaite K, Aylward LL *et al*. Serum concentration trends and apparent half-lives of per- and polyfluoroalkyl substances (PFAS) in Australian firefighters. *Int J Hyg Environ Health* 2022;**246**:114040.
15. Behnisch PA, Besselink H, Weber R *et al*. Developing potency factors for thyroid hormone disruption by PFASs using TTR-TRβ CALUX® bioassay and assessment of PFASs mixtures in technical products. *Environ Int* 2021;**157**:106791.
16. Blake BE, Rickard BP, Fenton SE. A high-throughput toxicity screen of 42 per- and polyfluoroalkyl substances (PFAS) and functional assessment of migration and gene expression in human placental trophoblast cells. *Front Toxicol* 2022;**4**:881347.
17. Bangma J, Eaves LA, Oldenburg K *et al*. Identifying risk factors for levels of per- and polyfluoroalkyl substances (PFAS) in the placenta in a high-risk pregnancy cohort in North Carolina. *Environ Sci Technol* 2020;**54**:8158–66.
18. Hall SM, Zhang S, Hoffman K *et al*. Concentrations of per- and polyfluoroalkyl substances (PFAS) in human placental tissues and associations with birth outcomes. *Chemosphere* 2022;**295**:133873.
19. Sagiv SK, Rifas-Shiman SL, Fleisch AF *et al*. Early-pregnancy plasma concentrations of perfluoroalkyl substances and birth outcomes in project viva: confounded by pregnancy hemodynamics?. *Am J Epidemiol* 2018;**187**:793–802.
20. Bach CC, Bech BH, Brix N *et al*. Perfluoroalkyl and polyfluoroalkyl substances and human fetal growth: a systematic review. *Crit Rev Toxicol* 2015;**45**:53–67.
21. Mora AM, Oken E, Rifas-Shiman SL *et al*. Prenatal exposure to perfluoroalkyl substances and adiposity in early and mid-childhood. *Environ Health Perspect* 2017;**125**:467–73.
22. Halldorsson TI, Rytter D, Haug LS *et al*. Prenatal exposure to perfluorooctanoate and risk of overweight at 20 years of age: a prospective cohort study. *Environ Health Perspect* 2012;**120**:668–73.
23. Starling AP, Liu C, Shen G *et al*. Prenatal exposure to per- and polyfluoroalkyl substances, umbilical cord blood DNA methylation, and cardio-metabolic indicators in newborns: the healthy start study. *Environ Health Perspect* 2020;**128**:127014.
24. Papadopoulou E, Stratakis N, Basagaña X *et al*. Prenatal and postnatal exposure to PFAS and cardiometabolic factors and inflammation status in children from six European cohorts. *Environ Int* 2021;**157**:106853.
25. Tian Y, Miao M, Ji H *et al*. Prenatal exposure to perfluoroalkyl substances and cord plasma lipid concentrations. *Environ Pollut* 2021;**268**:115426.
26. Pennings JL, Jennen DGJ, Nygaard UC *et al*. Cord blood gene expression supports that prenatal exposure to perfluoroalkyl substances causes depressed immune functionality in early childhood. *J Immunotoxicol* 2016;**13**:173–80.
27. Ames JL, Burjak M, Avalos LA *et al*. Prenatal exposure to per- and polyfluoroalkyl substances and childhood autism-related outcomes. *Epidemiology* 2023;**34**:450–9.
28. Goodman CV, Till C, Green R *et al*. Prenatal exposure to legacy PFAS and neurodevelopment in preschool-aged Canadian children: the MIREC cohort. *Neurotoxicol Teratol* 2023;**98**:107181.
29. Wang H, Luo F, Zhang Y *et al*. Prenatal exposure to perfluoroalkyl substances and child intelligence quotient: evidence from the Shanghai birth cohort. *Environ Int* 2023;**174**:107912.
30. Xie Z, Liang H, Miao M *et al*. Prenatal exposure to perfluoroalkyl substances and cognitive and neurobehavioral development in children at 6 years of age. *Environ Sci Technol* 2023;**57**:8213–24.
31. Jones PA. Functions of DNA methylation: islands, start sites, gene bodies and beyond. *Nat Rev Genet* 2012;**13**:484–92.
32. Reik W, Dean W, Walter J. Epigenetic reprogramming in mammalian development. *Science* 2001;**293**:1089–93.
33. Kim S, Thapar I, Brooks BW. Epigenetic changes by per- and polyfluoroalkyl substances (PFAS). *Environ Pollut* 2021;**279**:116929.
34. Perng W, Nakiwala D, Goodrich JM. What happens in utero does not stay in utero: a review of evidence for prenatal epigenetic programming by per- and polyfluoroalkyl substances (PFAS) in infants, children, and adolescents. *Curr Environ Health Rep* 2022;**10**:35–44.
35. Robinson SL, Zeng X, Guan W *et al*. Perfluorooctanoic acid (PFOA) or perfluorooctane sulfonate (PFOS) and DNA methylation in newborn dried blood spots in the Upstate KIDS cohort. *Environ Res* 2021;**194**:110668.
36. Liu Y, Eliot MN, Papandonatos GD *et al*. Gestational perfluoroalkyl substance exposure and DNA methylation at birth and 12 years of age: a longitudinal epigenome-wide association study. *Environ Health Perspect* 2022;**130**:037005.
37. Guibert S, Weber M. Functions of DNA methylation and hydroxymethylation in mammalian development. *Curr Top Dev Biol* 2013;**104**:47–83.
38. Petroff RL, Cavalcante RG, Langen ES *et al*. Mediation effects of DNA methylation and hydroxymethylation on birth outcomes after prenatal per- and polyfluoroalkyl substances (PFAS) exposure in the Michigan mother–infant pairs cohort. *Clin Epigenetics* 2023;**15**:49.
39. Jacobson LP, Lau B, Catellier D *et al*. An Environmental influences on Child Health Outcomes viewpoint of data analysis centers for collaborative study designs. *Curr Opin Pediatr* 2018;**30**: 269–75.
40. Blackwell CK, Wakschlag LS, Gershon RC *et al*. Measurement framework for the Environmental influences on Child Health Outcomes research program. *Curr Opin Pediatr* 2018;**30**: 276–84.
41. Bush NR, Wakschlag LS, LeWinn KZ *et al*. Family environment, neurodevelopmental risk, and the Environmental influences on Child Health Outcomes (ECHO) initiative: looking back and moving forward. *Front Psychiatry* 2020;**11**:547.
42. Gillman MW, Blaisdell CJ. Environmental influences on Child Health Outcomes, a research program of the National Institutes of Health. *Curr Opin Pediatr* 2018;**30**:260–2.
43. Knapp EA, Kress AM, Parker CB *et al*. The Environmental Influences on Child Health Outcomes (ECHO)-wide cohort. *Am J Epidemiol* 2023;**192**:1249–63.
44. Blaisdell CJ, Park C, Hanspal M *et al*. The NIH ECHO program: investigating how early environmental influences affect child health. *Pediatr Res* 2022;**92**:1215–6.
45. Goodrich JM, Ingle ME, Domino SE *et al*. First trimester maternal exposures to endocrine disrupting chemicals and metals and fetal size in the Michigan mother–infant pairs study. *J Dev Orig Health Dis* 2019;**10**:447–58.
46. Petroff RL, Padmanabhan V, Dolinoy DC *et al*. Prenatal exposures to common phthalates and prevalent phthalate alternatives and infant DNA methylation at birth. *Front Genet* 2022;**13**: 793278.
47. Padula AM, Ning X, Bakre S *et al*. Birth outcomes in relation to prenatal exposure to per- and polyfluoroalkyl substances and stress in the Environmental influences on Child Health Outcomes (ECHO) program. *Environ Health Perspect* 2023;**131**:37006.
48. Ladd-Acosta C, Vang E, Barrett ES *et al*. Analysis of pregnancy complications and epigenetic gestational age of newborns. *JAMA Network Open* 2023;**6**:e230672.

49. Andrews SV, Sheppard B, Windham GC *et al*. Case-control meta-analysis of blood DNA methylation and autism spectrum disorder. *Mol Autism* 2018;**9**:40.
50. Willer CJ, Li Y, Abecasis GR. METAL: fast and efficient meta-analysis of genomewide association scans. *Bioinformatics* 2010;**26**:2190–1.
51. Korthauer K, Kimes PK, Duvallet C *et al*. A practical guide to methods controlling false discoveries in computational biology. *Genome Biol* 2019;**20**:118.
52. Xu Z, Xie C, Taylor JA *et al*. ipDMR: identification of differentially methylated regions with interval P-values. *Bioinformatics* 2021;**37**:711–3.
53. Maksimovic J, Oshlack A, Phipson B. Gene set enrichment analysis for genome-wide DNA methylation data. *Genome Biol* 2021;**22**:173.
54. Davis AP, Wiegers TC, Johnson RJ *et al*. Comparative toxicogenomics database (CTD): update 2023. *Nucleic Acids Res* 2023;**51**:D1257–d1262.
55. Fang L, Zhang M, Li Y *et al*. PPARgene: a database of experimentally verified and computationally predicted PPAR target genes. *PPAR Res* 2016;**2016**:6042162.
56. Li C-H, Ren XM, Cao LY *et al*. Investigation of binding and activity of perfluoroalkyl substances to the human peroxisome proliferator-activated receptor β/δ. *Environ Sci Processes Impacts* 2019;**21**:1908–14.
57. Azhagiya Singam ER, Durkin KA, La Merrill MA *et al*. Prediction of the interactions of a large number of per- and polyfluoroalkyl substances with ten nuclear receptors. *Environ Sci Technol* 2024;**58**:4487–99.
58. Behr A-C, Plinsch C, Braeuning A *et al*. Activation of human nuclear receptors by perfluoroalkylated substances (PFAS). *Toxicol in Vitro* 2020;**62**:104700.
59. Miura R, Araki A, Miyashita C *et al*. An epigenome-wide study of cord blood DNA methylations in relation to prenatal perfluoroalkyl substance exposure: the Hokkaido study. *Environ Int* 2018;**115**:21–8.
60. Hu Q, Wu G, Ma H *et al*. Signal sequence receptor subunit 3: a novel indicator of immunosuppressive tumor microenvironment and clinical benefits from immunotherapy. *Cell Signal* 2023;**111**:110871.
61. Gerbracht JV, Boehm V, Britto-Borges T *et al*. CASC3 promotes transcriptome-wide activation of nonsense-mediated decay by the exon junction complex. *Nucleic Acids Res* 2020;**48**:8626–44.
62. Zhang Y, Lv J, Fan Y-J *et al*. Evaluating the effect of gestational exposure to perfluorohexane sulfonate on placental development in mice combining alternative splicing and gene expression analyses. *Environ Health Perspect* 2023;**131**:117011.
63. Izquierdo AG, Crujeiras AB, Casanueva FF *et al*. Leptin, obesity, and leptin resistance: where are we 25 years later?. *Nutrients* 2019;**11**:2704.
64. Qi W, Clark JM, Timme-Laragy AR *et al*. Per- and polyfluoroalkyl substances and obesity, type 2 diabetes and non-alcoholic fatty liver disease: a review of epidemiologic findings. *Toxicol Environ Chem* 2020;**102**:1–36.
65. Louisse J, Rijkers D, Stoopen G *et al*. Perfluorooctanoic acid (PFOA), perfluorooctane sulfonic acid (PFOS), and perfluorononanoic acid (PFNA) increase triglyceride levels and decrease cholesterogenic gene expression in human HepaRG liver cells. *Arch Toxicol* 2020;**94**:3137–55.
66. Deng P, Durham J, Liu J *et al*. Metabolomic, lipidomic, transcriptomic, and metagenomic analyses in mice exposed to pfos and fed soluble and insoluble dietary fibers. *Environ Health Perspect* 2022;**130**:117003.
67. Cassone CG, Taylor JJ, O'Brien JM *et al*. Transcriptional profiles in the cerebral hemisphere of chicken embryos following in ovo perfluorohexane sulfonate exposure. *Toxicol Sci* 2012;**129**:380–91.
68. Martin EM, Fry RC. A cross-study analysis of prenatal exposures to environmental contaminants and the epigenome: support for stress-responsive transcription factor occupancy as a mediator of gene-specific CpG methylation patterning. *Environ Epigenet*. 2016;**2**:dvv011.
69. Rampersaud A, Lodato NJ, Shin A *et al*. Widespread epigenetic changes to the enhancer landscape of mouse liver induced by a specific xenobiotic agonist ligand of the nuclear receptor CAR. *Toxicol Sci* 2019;**171**:315–38.
70. Diamant I, Clarke DB, Evangelista J *et al*. Harmonizome 3.0: integrated knowledge about genes and proteins from diverse multi-omics resources. *Nucleic Acids Res* 2025;**53**:D1016–28.
71. Rouillard AD, Gundersen GW, Fernandez NF *et al*. The harmonizome: a collection of processed datasets gathered to serve and mine knowledge about genes and proteins. *Database (Oxford)* 2016;**2016**:baw100.
72. Bastard J-P, Hainque B, Dusserre E *et al*. Peroxisome proliferator activated receptor-γ, leptin and tumor necrosis factor-α mRNA expression during very low calorie diet in subcutaneous adipose tissue in obese women. *Diabetes Metab Res Rev* 1999;**15**:92–8.
73. Zhang Y, Dallner OS, Nakadai T *et al*. A noncanonical PPARγ/RXRα-binding sequence regulates leptin expression in response to changes in adipose tissue mass. *Proc Natl Acad Sci U S A* 2018;**115**:E6039–47.
74. Rashid F, Ramakrishnan A, Fields C *et al*. Acute PFOA exposure promotes epigenomic alterations in mouse kidney tissues. *Toxicol Rep* 2020;**7**:125–32.
75. Wen Y, Mirji N, Irudayaraj J. Epigenetic toxicity of PFOA and GenX in HepG2 cells and their role in lipid metabolism. *Toxicol in Vitro* 2020;**65**:104797.
76. Taibl KR, Schantz S, Aung MT *et al*. Associations of per- and polyfluoroalkyl substances (PFAS) and their mixture with oxidative stress biomarkers during pregnancy. *Environ Int* 2022;**169**:107541.
77. Temkin AM, Hocevar BA, Andrews DQ *et al*. Application of the key characteristics of carcinogens to per and polyfluoroalkyl substances. *Int J Environ Res Public Health* 2020;**17**:1668.


Environmental Epigenetics, 2025, 11(1), dvaf010 , DOI: https://doi.org/10.1093/eep/dvaf010, Advance Access Publication 24 April 2025, Research Article
Received 7 August 2024; Revised 6 February 2025; Accepted 21 April 2025